Draft version February 1, 2008
Preprint typeset using LaTeX style emulateapj v. 04/03/99

BEPPOSAX OBSERVATIONS OF GRB980425: DETECTION OF THE PROMPT EVENT AND MONITORING OF THE ERROR BOX

E. Pian[1], L. Amati[1], L. A. Antonelli[2], R. C. Butler[1], E. Costa[3], G. Cusumano[4], J. Danziger[5], M. Feroci[3], F. Fiore[6], F. Frontera[1,7], P. Giommi[6], N. Masetti[1], J. M. Muller[6], L. Nicastro[4], T. Oosterbroek[8], M. Orlandini[1], A. Owens[8], E. Palazzi[1], A. Parmar[8], L. Piro[3], J. J. M. in 't Zand[9], A. Castro-Tirado[10], A. Coletta[6], D. Dal Fiume[1], S. Del Sordo[4], J. Heise[9], P. Soffitta[3], V. Torroni[6]

Draft version February 1, 2008

ABSTRACT

We present BeppoSAX follow-up observations of GRB980425 obtained with the Narrow Field Instruments (NFI) in April, May, and November 1998. The first NFI observation has detected within the 8′ radius error box of the GRB an X-ray source positionally consistent with the supernova 1998bw, which exploded within a day of GRB980425, and a fainter X-ray source, not consistent with the position of the supernova. The former source is detected in the following NFI pointings and exhibits a decline of a factor of two in six months. If it is associated with SN 1998bw, this is the first detection of X-ray emission from a Type I supernova above 2 keV. The latter source exhibits only marginally significant variability. The X-ray spectra and variability of the supernova are compared with thermal and non-thermal models of supernova high energy emission. Based on the BeppoSAX data, it is not possible to firmly establish which of the two detected sources is the GRB X-ray counterpart, although probability considerations favor the supernova.

Subject headings: gamma rays: bursts — Supernovae: individual: SN 1998bw

1. INTRODUCTION

The GRB of 1998 April 25, detected both by the BeppoSAX GRBM and by BATSE (Kippen 1998) and localized with arcminute accuracy by the BeppoSAX WFC (Soffitta et al. 1998), has received particular attention from the astronomers because of its spatial (within a few arcminutes) and temporal (within one day) consistency with the optically and radio exceedingly bright Type Ic supernova 1998bw (Galama et al. 1998; Kulkarni et al. 1998a; Iwamoto et al. 1998), in the nearby galaxy ESO 184-G82 ($z = 0.0085$, Tinney et al. 1998). The low probability of a chance coincidence between the two events ($\sim 10^{-4}$, Galama et al. 1998) has strengthened the hypothesis of a physical association between GRB980425 and the supernova.

However, since the other GRBs for which a redshift measurement is available are located at larger distances ($z \sim 0.7$ or higher) and are characterized by power-law decaying optical afterglows (Fruchter et al. 1999a; Djorgovski et al. 1997; Fruchter et al. 1999b; Halpern et al. 1998; Kulkarni et al. 1998b; Bloom et al. 1998a; Vreeswijk et al. 1999; Castro-Tirado et al. 1999; Galama et al. 1999a; Kulkarni et al. 1999; Fruchter et al. 1999c; Harrison et al. 1999; Stanek et al. 1999; Bakos et al. 1999), in agreement with the "classical" fireball model (e.g., Rees & Mészáros 1992; Piran 1999), GRB980425 has been regarded as a possible representative of a separate GRB class, with apparently indistinguishable high energy characteristics, but with different progenitors.

The existence of a particular class of GRBs and its possible association with supernovae have been systematically searched for using BATSE catalogs and supernovae compilations by several authors (Wang & Wheeler 1998; Norris et al. 1998; Bloom et al. 1998b; Kippen et al. 1998) or based on individual cases of supernovae with outstanding optical properties (Germany et al. 1999; Turatto et al. 1999; Terlevich, Fabian, & Turatto 1999).

Following the detection of GRB980425, observations of its WFC error box with the BeppoSAX Narrow Field Instruments (NFI) were immediately activated, starting 10 hours and one week after the event. The detection of two previously unknown X-ray sources - one of which being consistent with the position of the supernova, and the other possibly, but not clearly, fading - was regarded as quite anomalous, because previous BeppoSAX NFI follow-up observations of well localized GRBs had generally detected X-ray transients characterized by power-law decay. This fact prompted further observations six months after the event, aimed at clarifying the uncertainty about the

[1]Istituto Te.S.R.E., CNR, via Gobetti 101, I-40129 Bologna, Italy
[2]Osservatorio Astronomico di Roma, sede di Monteporzio Catone, Via Frascati 33, I-00040 Monteporzio Catone, Italy
[3]I.A.S., C.N.R., Via Fosso del Cavaliere, Area della Ricerca di Tor Vergata, I-00131 Rome, Italy
[4]I.F.C.A.I., CNR, via Ugo La Malfa 153, I-90146 Palermo, Italy
[5]Osservatorio Astronomico di Trieste, Via G.B. Tiepolo 11, I-34131 Trieste, Italy
[6]BeppoSAX Scientific Data Center, Via Corcolle 19, I-00131 Rome, Italy
[7]Physics Department, University of Ferrara, Via Paradiso, 12, I-44100 Ferrara, Italy
[8]Astrophysics Division, SSD of ESA, ESTEC, P.O. Box 299, 2200 AG Noordwijk, The Netherlands
[9]Space Research Organization Netherlands, Sorbonnelaan 2, 3584 CA Utrecht, The Netherlands
[10]IAA-CSIC, Granada, Spain and LAEFF-INTA, Madrid, Spain

GRB X-ray counterpart, and, as a secondary though not less important scope, at monitoring the X-ray emission of SN 1998bw, considering the peculiarity of this object and the poor knowledge of the X-ray behavior in supernovae in general (see review by Schlegel 1995), and particularly of Type I.

In this Letter we present the high energy characteristics of the prompt event as measured by the BeppoSAX GRBM and WFC, and the results of the follow-up NFI observations (§2) and discuss their implications in view of the detection of SN 1998bw in the GRB field (§3). A preliminary report on these data has been given in Pian et al. (1999).

2. DATA ANALYSIS AND RESULTS

2.1. *Prompt event*

GRB980425 triggered the BeppoSAX GRBM at 21:49:11 UT, and was simultaneously detected by the BeppoSAX WFC unit 2 (Soffitta et al. 1998). The event had a duration of 31 s in the range 40-700 keV and 40 s in the range 2-26 keV. It exhibited a single, non structured peak profile in both bands, with the indication of a ∼5 s soft lag (Fig. 1). Some flux brightening and successive decrease, lasting altogether ∼10 seconds, are seen in the WFC light curve after the first 40 seconds, but not in the γ-rays.

The GRBM and WFC light curves appear well correlated, with the indication of a ∼5 seconds lag of the lower energies with respect to the higher energies. Figure 2 shows the Discrete Correlation Function (DCF) between the two light curves. This correlation method is suited to search for correlations and temporal lags between two discrete, and possibly unevenly sampled, data trains (Edelson & Krolik 1988). To a maximum of the DCF amplitude at a positive temporal lag corresponds a positive correlation, with the higher energies leading the lower ones. A maximum at a positive temporal lag of ∼5 seconds is evident. The asymmetric shape of the DCF function amplitude around its peak reflects the fact that the flux decay after maximum is slower at X-rays than at γ-rays (see Fig. 1).

The fluences are $(2.8 \pm 0.5) \times 10^{-6}$ erg cm^{-2} and $(1.8 \pm 0.3) \times 10^{-6}$ erg cm^{-2} in the 40-700 keV and 2-26 keV energy range, respectively. (The Galactic absorption in the direction of GRB980425, $N_{HI} = 4 \times 10^{20}$ cm^{-2}, from Schlegel, Finkbeiner, & Davis 1998, is negligible at energies higher than 2 keV.) The spectral index of the γ-ray spectrum, averaged over the burst duration, is $\alpha = 1.2 \pm 0.2$ ($f_\nu \propto \nu^{-\alpha}$), and that of the X-ray spectrum is $\alpha = 0.41 \pm 0.25$. Strong spectral softening is evident during the event (Frontera et al. 1999). No peculiar temporal or spectral characteristics are noted in this GRB.

The spacecraft aspect reconstruction conditions allowed us to only poorly constrain the WFC error box of the GRB, which has a radius of 8′. This made the search of an X-ray transient more difficult. The IPN allowed a substantial reduction of the GRB error box (see Galama et al. 1999b).

2.2. *NFI Target of Opportunity Observations*

The BeppoSAX NFI were pointed at the 8′ radius error box determined by the WFC at three epochs starting 10 hours after the GRB: April 26-28, May 2-3 and November 10-12 (see Journal of Observations in Table 1; note that the April pointing was uninterrupted, but has been split in two parts only for the data analysis purpose). The strategy of performing NFI pointings at so large time intervals after the GRB (one week and six months), besides promptly thereafter, is not usually adopted for GRBs and was dictated by the ambiguity of the results obtained with the April observation, which suggested a quite different case than previously observed X-ray afterglows.

Event files for the LECS and MECS experiments were linearized and cleaned with SAXDAS at the BeppoSAX Science Data Center (SDC; Giommi & Fiore 1998). LECS (0.1-4 keV) and MECS (unit 2 and 3, 1.6-10 keV) images for each pointing were extracted using the XIMAGE software package. The MECS images, better exposed and of higher signal-to-noise ratio than the LECS ones, are reported in Fig. 3.

The analysis of the MECS imaging data of the first portion of the first pointing (Fig. 3a) shows that inside the intersection of the WFC error circle and IPN annulus, two point-like, previously unknown X-ray sources are detected with a positional uncertainty of 1′.5: 1SAXJ1935.0-5248 (hereafter S1), at RA = 19h 35m 05.9s and Dec = –52° 50′ 03″, and 1SAXJ1935.3-5252 (hereafter S2), at RA = 19h 35m 22.9s and Dec = –52° 53′ 49″. Note that the coordinates distributed by Pian et al. (1998) have been revised in November 1998, to take into account a systematic error due to the non-optimal spacecraft attitude during the April and May 1998 observations (see Piro et al. 1998a). The revised position of S1 is consistent within the uncertainty with the position of SN 1998bw detected in the WFC error box (Galama et al. 1998; Kulkarni et al. 1998a) and exploded simultaneously with the GRB with an uncertainty of ∼1 day (Iwamoto et al. 1998), while the revised position of S2 is ∼ 4′.5 away from SN 1998bw, and therefore inconsistent with it (see Fig. 1 in Galama et al. 1999b).

The LECS and MECS count rates and upper limits for both sources during the three pointings have been computed within circles of 3′ radius and corrected for the local background estimated within circles of similar size (Table 1). The upper limits have been estimated as explained in the Appendix. This method takes into account, in addition to the normal photon statistics, also the fact that, at these flux levels, the LECS and MECS background may be dominated by the fluctuations of the cosmic X-ray background.

Source S1 is detected by the MECS also in the following pointings at a position consistent with that of the first observation. The observation of November 1998 shows a decrease in the X-ray flux of approximately a factor of two with respect to the level measured in April-May 1998. The source is also detected by the LECS in the April pointing, and not in the November pointing (LECS data of the May 1998 pointing are excluded from the analysis because of the extremely short exposure time).

Due to the limited spatial resolution of the LECS and MECS detectors and to the faint emission level of source S2, estimating its flux is made difficult by the background contamination and by the proximity of the brighter source S1. During the second portion of the April pointing, as well as in the November 1998 pointing, S2 is not detected by the MECS, while signal from a position consistent with that of S2 in April is marginally detected in the May 1998

pointing (Fig. 3c), with lower flux than in the first observation (see Table 1), but consistent with it at the $\sim$2-σ level. We note that the May detection, albeit of a signal-to-noise formally lower than 3, has a very low probability of being a background fluctuation ($\sim 10^{-6}$) when considered together with the April detection. However, we conservatively report in Table 1 also the 3-σ upper limit for the May measurement. All upper limits to the flux of S2 are consistent with the level of the detection. There is no significant detection of S2 in the individual LECS images.

No significant signal above background is detected by the BeppoSAX high energy instruments PDS and HPGSPC in any of the three pointings.

Light curves and spectra for each pointing were accumulated with the XSELECT tool, using a 3 arcmin extraction radius both for the LECS and the MECS, which provides only 80% of flux, but allows partially avoiding the mutual contamination of S1 and S2. Since the local background intensity is similar to that measured from files accumulated from blank fields available at the SDC, we used the latter, which are affected by a smaller uncertainty. No significant variability within each pointing is exhibited by either source.

Spectral analysis of the LECS and MECS data has been done with the XSPEC 10.0 package using the response matrices and auxiliary files available at the SDC. LECS and MECS spectra flux distributions of both sources have been grouped in order to achieve a signal-to-noise ratio of at least $\sim$3 in each bin.

For S1, a fit with a single power-law ($F_\nu \propto \nu^{-\alpha}$) absorbed by Galactic extinction of the individual MECS spectra is satisfactory, with reduced χ^2 values well below one, due to the large errors. For these fits at individual epochs the LECS spectra have not been used because they have too low signal-to-noise ratio.

Since no significant spectral variability is seen from epoch to epoch, we averaged the LECS and MECS spectra of April and May, to increase the signal-to-noise ratio, and fitted a single power-law to the average rebinned spectrum. We excluded the November spectrum from this average because the count rates indicate that the flux varied at that epoch with respect to April-May (Table 1).

We obtain a spectral index of $\alpha = 1.0 \pm 0.3$ (all fit parameters for the average spectrum are reported in Table 2). The fitted N_{HI} is found to be consistent with the Galactic value and therefore we have fixed it to that value. The intercalibration constant between the LECS and MECS data is within the expected range. However, the fit is formally not completely satisfactory (reduced $\chi^2 = 1.2$, see Table 2), due to a flux excess at energies below $\sim$ 1 keV (Fig. 4a).

We also tried a fit with a thermal bremsstrahlung with Galactic absorption, obtaining a temperature $kT \simeq 8$ keV and a not satisfactory reduced χ^2 of 1.7, still due to the presence of a soft excess (Fig 5a).

Fitting the data assuming no Galactic absorption still yields some soft excess with respect to both a power-law and a bremsstrahlung model, therefore we tend to exclude that the effect is due to an overestimate of the Galactic extinction in the direction of SN 1998bw (as possibly suggested by Patat et al. 1999).

A fit of the data with a broken power-law and Galactic absorption yields an index $\alpha_1 = 2.0 \pm 0.5$ below 1.4 keV and $\alpha_2 = 0.7 \pm 0.4$ at the higher energies. The reduced χ^2 is 0.5, considerably lower than for the single power-law and for the bremsstrahlung models (see Fig. 6).

To account for the soft excess we also tried composite fits of a power-law or a thermal bremsstrahlung with a black body model plus Galactic absorption. The former fit yields a spectral index $\alpha = 0.5 \pm 0.3$ and a black body temperature $kT = 90 \pm 20$ eV, with a reduced $\chi^2 = 0.5$ (Fig. 4b). The latter yields a bremsstrahlung temperature of $kT \sim 16$ keV (see Table 2), and black body temperature and normalization consistent with those found in the former case (reduced $\chi^2 = 0.5$, Fig. 5b).

We found no obvious reason for the excess to be spurious, such as instrumental effect or non optimal background subtraction. Therefore we considered it real, although not highly significant (see Figures 4a and 5a). The chance probabilities that adding a black body component either to a power-law or to a thermal bremsstrahlung model improves the fit are 1.3% and 0.17%, respectively. Fitting the data with a broken instead of a single power-law has a chance probability of improvement of 4%.

The low signal-to-noise ratio of the LECS data in November 1998 does not allow us to test the goodness of the fit of those data with a black body model. By fixing the black body temperature to the best fit value of the April-May spectrum, 90 eV, and fitting a power-law plus black body model to the November MECS spectrum and LECS upper limit we get a black body normalization upper limit consistent with the value obtained for April-May, indicating that this component has not varied significantly. The power-law normalization has instead varied by a factor of ~ 2.

Although there is no detection of S2 in the individual LECS images, signal is present in the April-May coadded image. Therefore, since the MECS spectra of the individual observations have a very low signal-to-noise ratio, we only used the rebinned LECS+MECS spectrum obtained from the average April-May image, and fitted it with a power-law of index $\alpha = 1.5 \pm 0.4$ plus Galactic absorption ($\chi^2 = 0.5$).

Due to the high uncertainty in the power-law spectral index and to the low level of both S1 and S2, we estimated their intensities in the 2-10 keV band by assuming a standard factor of conversion from count rates of 9.3×10^{-11}, corresponding to an adopted power-law spectral shape of index 0.5. The 1-σ uncertainties on the intensities have been obtained by similarly scaling the errors on the count rates (Table 1). These intensities are reported in Figure 7, along with the WFC light curve in the 2-10 keV band, obtained by binning in intervals of 5-20 seconds the temporal profile reported in Figure 1. Differences between these intensities and those obtained by adopting a bremsstrahlung model do not exceed 10%. Note that the contribution of the black body component to the intensity of S1 in the 2-10 keV range is negligible.

3. DISCUSSION

3.1. *Light curve and spectral shape of source S1*

The X-ray light curve of source S1 measured by the NFIs shows a decay of a factor of two in $\sim$6 months (Fig. 7b), much slower than X-ray GRB afterglows so far observed. Assuming, as suggested by the positional coincidence and

by variability, that S1 is associated with SN 1998bw, this is the first detection of medium energy X-ray emission from a Type I supernova (there is a unique case of Type I supernova detected in soft X-rays, the Type Ic SN 1994I, Immler et al. 1998a) and the earliest detection of X-rays after supernova explosion.

At the distance of SN 1998bw, 38 Mpc, the luminosity observed in the range 2-10 keV, $\sim 4 - 7 \times 10^{40}$ erg s^{-1}, would be compatible with that of other supernovae detected in the same energy band (Kohmura et al. 1994; Houck et al. 1998; Schlegel 1995, and references therein).

However, the observed luminosity and variation thereof represent only an upper limit to the luminosity and a lower limit to the amplitude of X-ray variability of SN 1998bw, respectively, due to the possible contribution of its host galaxy, a face-on spiral galaxy about one tenth of the size of our Galaxy, which is only very marginally resolved in the BeppoSAX data. In fact, a galaxy of that type and size could easily account for almost all of the X-ray emission observed in November 1998, when the flux was lowest (see e.g., Fabbiano 1989).

The observed decay of S1 in the 2-10 keV band is well fitted by a power-law $F(t) \propto t^{-p}$ with $p = 0.16 \pm 0.04$ (reduced $\chi^2 \simeq 0.7$). The fit with an exponential law $F(t) \propto e^{-t/\beta}$ with $\beta = 500 \pm 100$ days has a reduced χ^2 of 2.4, corresponding to a probability of ∼10% for 2 degrees of freedom, therefore not negligible (Fig. 7b). Both trends would be similar, considering the unknown dilution by the host galaxy of SN 1998bw, to the X-ray behavior of other supernovae (e.g., Kohmura et al. 1994; Zimmermann et al. 1994; Houck et al. 1998) and predicted by models of thermal bremsstrahlung of energetic electrons within the circumstellar medium (see e.g., Chevalier & Fransson 1994; Chugai & Danziger 1994).

The prompt X-ray emission observed for SN 1998bw requires that the circumstellar medium is highly ionized (perhaps by the powerful explosion), to allow the X-rays to escape so soon after the explosion (see Zimmermann et al. 1994), and also very dense, as inferred also from the large radio output (Kulkarni et al. 1998a; Wieringa, Kulkarni, & Frail 1999). In these conditions, the X-rays might be produced by the reverse shock which results from the pressure of swept-up material on the outgoing shock and propagates back into the shocked supernova gas (Chevalier & Fransson 1994; Schlegel 1995).

The temperature obtained from the thermal bremsstrahlung fit to the BeppoSAX LECS+MECS spectra, admittedly very poorly constrained, is compatible with that fitted to the medium or hard X-ray spectra of other supernovae (Kohmura et al. 1994; Leising et al. 1994; Dotani et al. 1987).

On the other hand, the mildly relativistic conditions evidently present in the expanding shock of SN 1998bw at early epochs (Kulkarni et al. 1998a) and the acceptable power-law fit obtained for the medium energy X-ray spectra might suggest that non-thermal mechanisms are responsible for the X-ray emission such as synchrotron radiation by the extremely energetic electrons, as was modeled for the radio emission by Li and Chevalier (1999), or inverse Compton scattering of relativistic electrons off optical/UV photons of the thermal ejecta (see Canizares et al. 1982). The X-ray spectral index is consistent with that measured for the radio spectrum starting ∼ 15 days after the explosion (Kulkarni et al. 1998a; Wieringa et al. 1999), and with the slope connecting quasi-simultaneous radio and X-ray measurements ($\alpha \sim 0.8$). Therefore, it is difficult to establish whether the X-rays are produced through synchrotron or inverse Compton radiation. However, if inverse Compton losses were dominant, radio emission production would be rapidly inhibited (Schlegel 1995), contrary to the observations.

Assuming the X-rays have a synchrotron origin and adopting a single power-law of index $\alpha \sim 0.8$ for the radio-to-X-ray synchrotron spectrum, we obtain a bolometric luminosity of $\sim 9 \times 10^{40}$ erg s^{-1}. Assuming that the radio and X-ray emitting regions are cospatial and expanding with a speed of $\sim 0.3c$ (Kulkarni et al. 1998a), we derive a magnetic field of $\lesssim 1$ Gauss, similar to that found for SN 1980K by Canizares et al. (1982) assuming inverse Compton losses are responsible for the X-ray production.

However, the limited signal-to-noise ratio of the BeppoSAX spectra does not allow us to choose between synchrotron radiation and thermal bremsstrahlung as the mechanism for the medium energy X-ray production.

The emission component detected in the softer part of the BeppoSAX spectrum, if fitted with a black body, has a temperature of ∼0.1 keV, corresponding to a black body total luminosity of $\sim 10^{41}$ erg s^{-1}. The inferred linear size of the emitting region is about one third of the solar radius, too large for a compact object left as a remnant of the supernova explosion, but approximately compatible with the size of the putative accretion disk promptly formed as a consequence of the "hypernova" or "collapsar" phenomenon, of which SN 1998bw might be an example (Paczyński 1998; MacFadyen & Woosley 1998; Woosley, Eastman, & Schmidt 1999a). However, such a compact object or disk could be hardly visible at a so early epoch, due to the optical thickness of the material enshrouding it.

Black body soft X-ray emission is not expected from the supernova itself or from the expanding shell or ejecta, due to non-equilibrium conditions of the system. However, the occurrence of short (∼1000 s) thermal bursts at early times after supernova explosion has been predicted, albeit at very soft energies, possibly even lower than those observable by the LECS (Schlegel 1995). We found no evidence in the LECS light curves of similar events, but the sampling is not conducive to that detection.

However, since there is no evidence of variability of the soft component in the long term, it might not be related to the supernova. In fact, its spectrum can be fitted also with a power-law superimposed on, and steeper than, the one which describes the spectrum at higher energies. This suggests that the component might have a more complex spectrum (possibly extending toward ultraviolet wavelengths), of which a black body or steep power-law are only approximations. It could rather be a persistent (or slowly variable with a small amplitude) source of soft X-rays such as the host galaxy itself, or just its bulge, or the superposition of unresolved X-ray sources within that galaxy, or diffuse hot gas, or the HII region in which SN 1998bw is located (Galama et al. 1998), or the underlying cluster DN 1931-529, or more probably, the sum of some or all of these contributions. The limited angular resolution of BeppoSAX does not allow us to disentangle this component from the

supernova itself. Notwithstanding this possibility, we note that the unabsorbed luminosity in the 0.1-2 keV range, 5×10^{40} erg s^{-1}, given by the superposition of the fitted power-law and black body components, is similar to luminosities of supernovae observed in soft X-rays (Canizares et al. 1982; Bregman & Pildis 1992; Zimmermann et al. 1994; Schlegel et al. 1996; Fabian & Terlevich 1996; Immler et al. 1998b).

3.2. *The association between GRB980425 and SN 1998bw*

The GRB980425 prompt event is relatively weak with respect to other GRBs, and rather soft. However, it has no outstanding features with respect to other BeppoSAX or BATSE GRBs, which might suggest a peculiar counterpart at longer wavelengths, such as a bright supernova, instead of a "classical" power-law fading afterglow. The ∼5-seconds temporal lag between the WFC and the GRBM light curves could be due to a delay of X-ray emission during the burst with respect to the γ-rays, or ascribed to intrinsic absorption in a medium becoming increasingly transparent (see e.g., Böttcher et al. 1999). Similar soft lags from few to ∼10 seconds are observed also in other GRBs (Piro et al. 1998b; Piro et al. 1998c; Frontera et al. 1999).

If SN 1998bw is the counterpart of GRB980425, the production of γ-rays could be accounted for by the explosion of the 14 $M_\odot$ helium core of a $\sim 35\ M_\odot$ star (Woosley et al. 1999a; MacFadyen & Woosley 1999) and by the subsequent expansion of a relativistic shock, in which non-thermal electrons are radiating photons of ∼100 keV, provided the explosion is asymmetric, i.e. the GRB is produced in a relativistic jet (Iwamoto et al. 1998; Woosley et al. 1999a; Höflich, Wheeler, & Wang 1999; Rej 1998; see however, Kulkarni et al. 1998a). The presence of an undetectable, or barely detectable, non-thermal GRB remnant, underlying the brighter thermal supernova ejecta cannot be excluded (see e.g., Iwamoto 1999).

Recent speculations have led to the proposal that every long (> 1 s) GRB is formed via supernova, or hypernova, explosion (MacFadyen & Woosley 1999). The presence of a supernova underlying the GRB afterglow has been recently tested for the optical transients of some GRBs with suggestive results (GRB970228, Reichart 1999; Galama et al. 1999c; GRB970508, Germany et al. 1999; GRB980326, Bloom et al. 1999; GRB990510, Fruchter et al. 1999d; Beuermann et al. 1999; GRB990712, Hjorth et al. 1999). Indeed, the recent discovery of a GRB optical counterpart at the intermediate redshift $z = 0.43$ (Galama et al. 1999d) might support a continuity of properties between GRB980425 and the other precisely localized GRBs, perhaps based on the different amount of jet collimation (Woosley, MacFadyen, & Heger 1999b) or different beaming, depending on the degree of jet alignment (Eichler & Levinson 1999; Cen 1998; Postnov, Prokhorov, & Lipunov 1999). In highly collimated or highly beamed GRBs the non-thermal multiwavelength afterglow could overwhelm the underlying supernova emission. This should instead be detected more clearly in less collimated or less beamed (i.e., seen off-axis) GRBs, like GRB980425, which are, or appear, weaker. Assuming association with SN 1998bw and isotropic emission, the total energy of GRB980425 in the 40-700 keV, $\sim 5 \times 10^{47}$ erg, is at least four orders of magnitude less than that of GRBs with known distance.

On the other hand, disregarding the fact that the probability of a chance coincidence of GRB980425 and SN 1998bw is extremely low, one might consider S2 as the X-ray counterpart candidate of the burst. The possible detection of S2 in 2-3 May 1998, one week after the GRB, implies, with respect to the first NFI detection in April, a much slower decay than that normally observed for X-ray afterglows (e.g., Costa et al. 1997; Nicastro et al. 1998; Dal Fiume et al. 1999; in 't Zand et al. 1998; Nicastro et al. 1999; Vreeswijk et al. 1999; Heise et al. 1999).

Assuming a power-law decay between the X-ray flux measured by the WFC in the 2-10 keV range in the last ∼20 seconds of the GRB and the flux measured in the first NFI observation (Fig. 7a), we derive a power-law index $p \sim 1.5$, which is similar to commonly observed X-ray afterglows. If S2 is an afterglow, one would expect that its intraday variability followed this same temporal behavior. Therefore, we have binned the light curve of S2 in the first portion of the April 1998 pointing in five intervals of 20000 seconds each. We have then connected with power-laws the last WFC measurement with the first and last of these fluxes and have determined their indices to be $p \simeq 1.6$ and $p \simeq 1.4$ (Fig. 7c), respectively. The reduced χ^2 values computed for these two power-laws with respect to the remainder four NFI data points of April are 3 and 30, respectively, corresponding to low probabilities (1% and $\ll$1) that the power-laws describe the observed intrapointing light curve. (All points seem rather consistent with a constant trend.)

The upper limit derived for the second portion of the April pointing is inconclusive. However, the detection of S2 in May 1998 suggests a marginal deviation from the above power-laws ($\gtrsim 2.5\sigma$). Therefore, the present data exclude at a confidence level of ∼99%, or higher, that S2 is an afterglow, unless a small re-bursting, one week after the GRB, is superimposed to the power-law monotonic decline. This would be reminiscent of GRB970508, although the time scales for re-bursting occurrence and duration would be very different (Piro et al. 1998b).

4. CONCLUSION

Two previously unknown X-ray sources have been detected by the BeppoSAX NFIs in the field of GRB980425. Neither of them has the obvious characteristics of an X-ray afterglow, when compared to previously observed cases.

SN 1998bw is a very interesting candidate for further monitoring in the X-rays. Thanks to its rapid slew capability and to its wide energy range, BeppoSAX has promptly measured its spectrum up to energies beyond ~ 5 keV, where supernovae have been so far largely unexplored. Unfortunately, the signal is relatively modest (this is the second most distant supernova detected so far in the X-rays, after SN 1988Z, located at 95 Mpc, Fabian & Terlevich 1996), and therefore longer exposures and data of better signal-to-noise ratio are necessary to study in detail this source and its environment.

Concerning the identification of the X-ray counterpart of GRB980425, our tentative conclusion is that S1 has a high probability of being associated with GRB980425, while S2 is more probably a variable field source, albeit constant in the long term, like an active galaxy or a Galactic X-ray bi-

nary (we note that the probability of detecting by chance a source of the level of S2 is rather high, $\sim$10%, Cagnoni et al. 1998; Giommi et al. 1998). A spectroscopic survey of the NFI error box of S2 has been inconclusive in this respect (Halpern 1998). Observations of this field by an X-ray instrument with higher sensitivity (e.g., XMM) and spatial resolution (e.g., Chandra) than those attained by BeppoSAX might help elucidating this controversial issue.

We thank the BeppoSAX Mission Planning Team and the BeppoSAX SDC and SOC personnel for help and support in the accomplishment of this project.

APPENDIX

ESTIMATE OF UPPER LIMITS AT 3-σ CONFIDENCE LEVEL

Suppose that m counts are found in the region where the target is expected to appear and that in the same search area b counts are expected from the background. If $m - b < 3\sqrt{b}$ we have no positive detection (at the 3-σ confidence level) of the source and a 3-σ upper limit is needed. We define the 3-σ upper limit as the number x that gives a probability to observe m or less counts equal to the formal 3-σ Gaussian probability, i.e.:

$$P(\leq m, x + b) = P_{Gauss}(3\sigma) \tag{1}$$

Assuming Poisson statistics, eq. (1) becomes:

$$e^{-(x+b)} \sum_{i=1}^{m} \frac{(x+b)}{i!} = 2.7 \times 10^{-3} \tag{2}$$

In the limit of large numbers eq. (2) reduces to

$$m = x + b - 3\sqrt{x + b} \tag{3}$$

By solving (3) with respect to x we have

$$x = \frac{9 + 2m + 3\sqrt{9 + 4m} - 2b}{2}.$$

REFERENCES

Bakos, G., Sahu, K., Menzies, J., Vreeswijk, P. M., & Frontera, F. 1999, GCN Circ. N. 387
Beuermann, K., et al. 1999, A&A, in press (astro-ph/9909043)
Bloom, J. S., et al. 1998a, ApJ, 508, L21
Bloom, J. S., et al. 1998b, ApJ, 506, L105
Bloom, J. S., et al. 1999, Nature, submitted (astro-ph/9905301)
Böttcher, M., Dermer, C. D., Crider, A. W., & Liang, E. P. 1999, A&A, 343, 111
Bregman, J. N., & Pildis, R. A. 1992, ApJ, 398, L107
Cagnoni, I., Della Ceca, R., & Maccacaro, T. 1998, ApJ, 493, 54
Canizares, C., Kriss, G., & Feigelson, E. D. 1982, ApJ, 253, L17
Castro-Tirado, A. J., et al. 1999, Science, 283, 2069
Cen, R. 1998, ApJ, 507, L131
Chevalier, R. A., & Fransson, C. 1994, ApJ, 420, 268
Chugai, N. N., & Danziger, I. J. 1994, MNRAS, 268, 173
Costa, E., et al. 1997, Nature, 387, 783
Dal Fiume, D., et al. 1999, A&A, submitted
Djorgovski, S. G., et al. 1997, Nature, 387, 876
Dotani, T., et al. 1987, Nature, 330, 230
Edelson, R., & Krolik, J. H. 1988, ApJ, 333, 646
Eichler, D., & Levinson, A. 1999, ApJ, 521, L117
Fabbiano, G. 1989, ARA&A, 27, 87
Fabian, A. C., & Terlevich, R. 1996, MNRAS, 280, L5
Frontera, F., et al. 1999, ApJ, submitted
Fruchter, A. S., et al. 1999a, ApJ, 516, 683
Fruchter, A. S., et al. 1999b, ApJ, in press (astro-ph/9903236)
Fruchter, A. S., et al. 1999c, ApJ, 519, L13
Fruchter, A. S., et al. 1999d, GCN Circ. N. 386
Galama, T. J., et al. 1998, Nature, 395, 670
Galama, T. J., et al., 1999a, Nature, 398, 394
Galama, T. J., et al. 1999b, A&AS, 138, 465
Galama, T. J., et al. 1999c, ApJ, submitted (astro-ph/9907264)
Galama, T. J., et al. 1999d, GCN Circ. N. 388
Germany, L., Reiss, D. J., Sadler, E. M., Schmidt, B. P., Stubbs, C. W. 1999, ApJ, submitted (astro-ph/9906096)
Giommi, P., & Fiore F. 1998, in The 5th International Workshop on Data Analysis in Astronomy, Erice, in press, Italy, eds. V. di Gesú, M.J.B. Duff, A. Heck, M.C. Maccarone, L. Scarsi, H.U. Zimmermann, World Scient. Publ., p. 73
Giommi, P., et al. 1998, Nuc. Phys. B (Proc. Suppl.) 69/1-3, 591
Halpern, J. P., Thorstensen, J. R., Helfand, D. J., & Costa, E. 1998, Nature, 393, 41
Halpern, J. P. 1998, GCN Circ. N. 156
Harrison, F. A., et al. 1999, ApJ, 523, L121
Heise, J., et al., 1999, IAU Circ. N. 7099
Hjorth, J., Fynbo, J., Dar, A., Courbin, F., & Moller, P. 1999, GCN Circ. N. 403
Höflich, P., Wheeler, J. C., & Wang, L. 1999, ApJ, 521, 179
Houck, J. C., Bregman, J. N., Chevalier, R. A., & Tomisaka, K., 1998, ApJ, 493, 431
Immler, S., Pietsch, W., & Aschenbach, B. 1998a, A&A, 336, L1
Immler, S., Pietsch, W., & Aschenbach, B. 1998b, A&A, 331, 601
Iwamoto, K., et al. 1998, Nature, 395, 672
Iwamoto, K. 1999, ApJ, 512, L47
Kippen, R. M., et al. 1998, ApJ, 506, L27
Kippen, R. M. 1998, GCN Circ. N. 67
Kohmura, Y., et al. 1994, PASJ, 46, L157
Kulkarni, S. R., et al. 1998a, Nature, 395, 663
Kulkarni, S. R., et al. 1998b, Nature, 393, 35
Kulkarni, S. R., et al. 1999, Nature, 398, 389
Leising, M. D., et al. 1994, ApJ, 431, L95
Li, Z.-Y., & Chevalier, R. A. 1999, ApJ, in press (astro-ph/9903483)
MacFadyen, A., & Woosley, S. E. 1999, ApJ, in press (astro-ph/9810274)
Nicastro, L., et al. 1998, A&A, 338, L17
Nicastro, L., et al. 1999, A&AS, 138, 437
Norris, J. P., Bonnell, J. T., & Watanabe, K. 1999, ApJ, 518, 901
Paczyński, B. 1998, ApJ, 494, L45
Patat, F., et al. 1999, in preparation
Pian, E., et al. 1998, GCN Circ. N. 61
Pian, E., et al. 1999, A&AS, 138, 463
Piran, T. 1999, Phys. Rep., 314, 575
Piro, L., et al. 1998a, GCN Circ. N. 155
Piro, L., et al. 1998b, A&A 331, L41
Piro, L., et al. 1998c, A&A, 329, 906
Postnov, K. A., Prokhorov, M. E., & Lipunov, V. M. 1999, A&A, in press (astro-ph/9908136)
Rees, M. J., & Mészáros, P. 1992, MNRAS, 258, 41
Reichart, D. E. 1999, ApJ, 521, L111
Rej, A. 1998, astro-ph/9810510
Schlegel, D. J., Finkbeiner, D. P., & Davis, M. 1998, ApJ, 500, 525
Schlegel, E. M. 1995, Rep. Prog. Phys., 58, 1375
Schlegel, E. M., Petre, R., & Colbert, E. J. M., 1996, ApJ, 456, 187
Soffitta, P., et al. 1998, IAU Circ. N. 6884
Stanek, K. Z., Garnavich, P. M., Kaluzny, J., Pych, W., Thompson, I. 1999, ApJ, 522, L39
Terlevich, R., Fabian, A., & Turatto, M. 1999, IAU Circ. N. 7269
Tinney, C., Stathakis, R., Cannon, R., & Galama, T. J. 1998, IAU Circ. N. 6896
Turatto, M., et al. 1999, in preparation
Vreeswijk, P. M., et al. 1999, ApJ, 523, 171
Wang, L., & Wheeler, J. C. 1998, ApJ, 504, L87
Wieringa, M. H., Kulkarni, S. R., & Frail, D. A. 1999, A&AS, 138, 467
Woosley, S. E., Eastman, R. G., & Schmidt, B. P. 1999a, ApJ, 516, 788
Woosley, S. E., MacFadyen, A., & Heger, A. 1999b, in: Supernovae and Gamma-Ray Bursts, The Largest Explosions Since the Big Bang, eds. M. Livio, K. Sahu, and N. Panagia (Cambridge: Cambridge University Press), in press (astro-ph/9909034)
in 't Zand, J. J. M., et al. 1998, ApJ 505, L119
Zimmermann, H.-U., et al. 1994, Nature, 367, 621

Table 1: Journal of BeppoSAX LECS and MECS Observations

Date (UT)	LECS			MECS		
	t[a] (s)	Flux[b]($\times 10^{-3}$ cts s^{-1})		t[a] (s)	Flux[c]($\times 10^{-3}$ cts s^{-1})	
		S1	S2		S1	S2
1998 Apr 26.334-27.458	24483	4.0 ± 1.3[d]	< 4.0	37220	4.6 ± 0.6	2.4 ± 0.5
Apr 27.469-28.160	13566	< 7.0	< 7.0	21805	4.5 ± 0.7	< 2.5
May 02.605-03.621	1016.5	–	–	31975	3.0 ± 0.5	1.4[e] ± 0.5
Nov 10.754-12.004	16961	< 6.0	< 6.0	53122	1.8 ± 0.4	< 2.0

[a] On source exposure time
[b] In the energy range 0.1-4 keV
[c] In the energy range 1.6-10 keV
[d] All uncertainties are at 1-σ; upper limits are at 3-σ
[e] The 3-σ upper limit is 1.9×10^{-3} cts s^{-1}

Table 2: Fits to the BeppoSAX LECS+MECS Average Spectrum of S1 in April-May 1998

Model	α_1	α_2	E_{break} keV	kT_{THB} keV	kT_{BB} eV	Red. χ^2	D.o.F.
Single Power-Law	1.0 ± 0.3	-	-	-	-	1.18	12
Thermal Bremsstrahlung	-	-	-	$7.5^{+13.5}_{-3.5}$	-	1.66	12
Broken Power-Law	2.0 ± 0.5	0.7 ± 0.4	1.4 ± 0.6	-	-	0.49	9
Power-Law + Black Body	0.5 ± 0.3	-	-	-	90^{+30}_{-20}	0.49	10
Th. Bremss. + Black Body	-	-	-	16^{+130}_{-10}	90^{+30}_{-20}	0.46	10

[a] Uncertainties are at 90% (1.6-σ) confidence level

FIG. A1.— BeppoSAX WFC (top) and GRBM (bottom) light curves of GRB980425. The onset of the GRB, indicated by the zero abscissa, corresponds to 1998 April 25.909097 (i.e., 5 seconds earlier than the GRBM trigger time). The vertical bars represent the typical 1-σ uncertainty associated with the individual flux points.

FIG. A2.— Discrete Correlation Function between WFC and GRBM light curves. The maximum at $\sim$5 seconds indicates positive correlation between the two curves with the WFC light curve lagging the GRBM one by that temporal lag.

FIG. A3.— BeppoSAX MECS images of the field of GRB980425 in the energy band 1.6-10 keV referring to the epochs: (a) 1998 April 26.334-27.458; (b) April 27.469-28.160; (c) May 2.605-3.621; (d) November 10.754-12.004. The local background has been subtracted and a smoothing has been applied with a window function of width comparable to the MECS detector point spread function ($3'$ at half power diameter). The source S1 is clearly seen in all images. The fainter source S2 is detected in the first part of the first pointing, panel (a), and in the May 1998 pointing, panel (c). Note that in May 1998, panel (c), the pointing center was significantly displaced with respect to the April pointing, which accounts for the presence of the bright source toward North-East, about $9'$ from the image center, not visible in panels (a) and (b). In each image, the most external contours represent 2-σ flux levels.

FIG. A4.— BeppoSAX LECS and MECS spectra of S1 fitted with (a) a single power-law and (b) a power-law plus black body. The lower panels show the ratios between the data and the model. See Table 2 for the fit parameters.

FIG. A5.— BeppoSAX LECS and MECS spectra of S1 fitted with (a) a thermal bremsstrahlung and (b) a thermal bremsstrahlung plus black body. The lower panels show the ratios between the data and the model. See Table 2 for the fit parameters.

FIG. A6.— BeppoSAX LECS and MECS spectra of S1 fitted with a broken power-law. The lower panel shows the ratios between the data and the model. See Table 2 for the fit parameters.

FIG. A7.— BeppoSAX MECS light curves in the 2-10 keV band of the X-ray sources S1 (open squares) and S2 (filled circles) detected in the GRB980425 field. The WFC early measurements in the same band are also shown (stars). Uncertainties for the NFI measurements are 1-σ. The 1-σ error bars for the WFC points are smaller than the symbol size and have not been reported. (b) Same as (a) for source S1 only. The fits to the temporal decay with a power-law of index ~ 0.2 and with an exponential law of e-folding time ~ 500 days are shown as dotted and dashed curves, respectively. (c) Same as (a) for source S2 only. The first NFI measurement of S2 in (a) is replaced here by 5 points obtained by integrating and averaging the flux in shorter time intervals. The dotted lines represent the power-laws of indices $p \simeq 1.6$ and $p \simeq 1.4$ connecting the last WFC measurement and the first and last of the 5 NFI points of the April 26-27 light curve, respectively. The extrapolations of the power-laws to the time of the third NFI observation (May 1998) fall below the lower bound of the data point, although they are compatible with it at the $\gtrsim 2.5\sigma$ level.

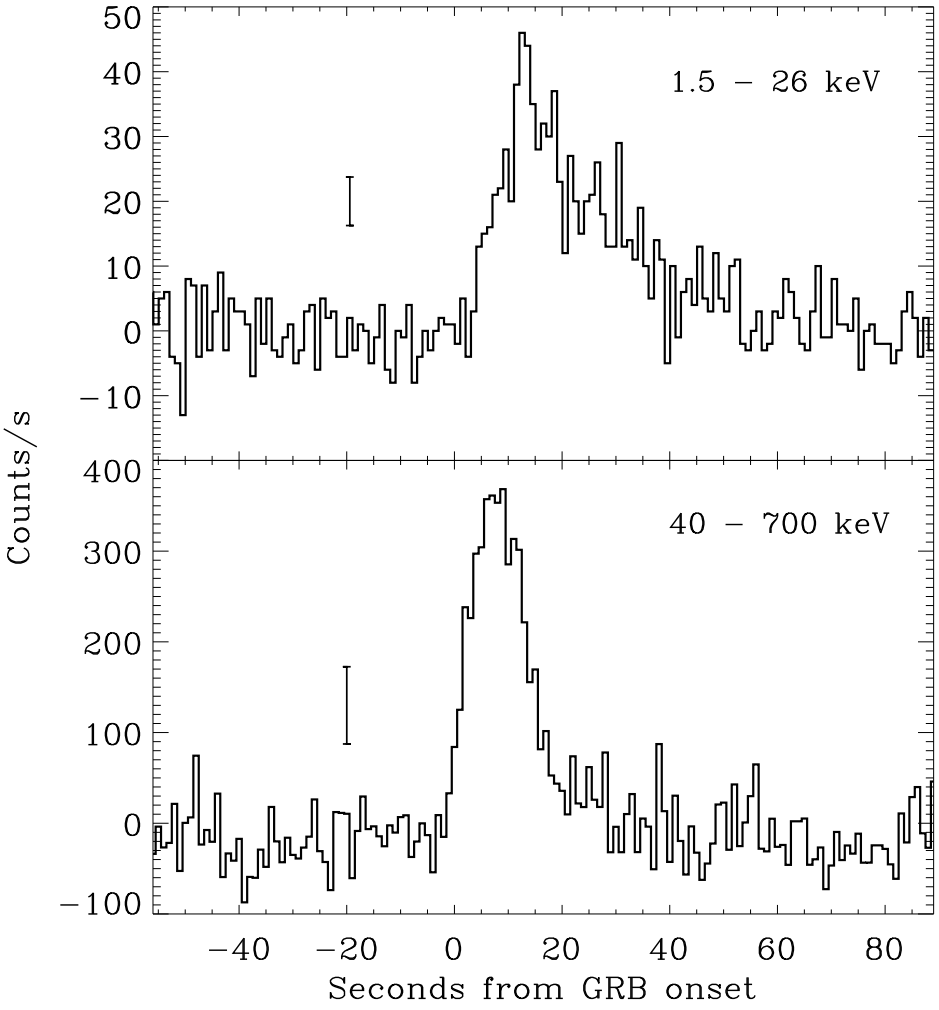

Fig. 1 – BeppoSAX WFC (top) and GRBM (bottom) light curves of GRB980425. The onset of the GRB, indicated by the zero abscissa, corresponds to 1998 April 25.909097 (i.e., 5 seconds earlier than the GRBM trigger time). The vertical bars represent the typical 1-σ uncertainty associated with the individual flux points.

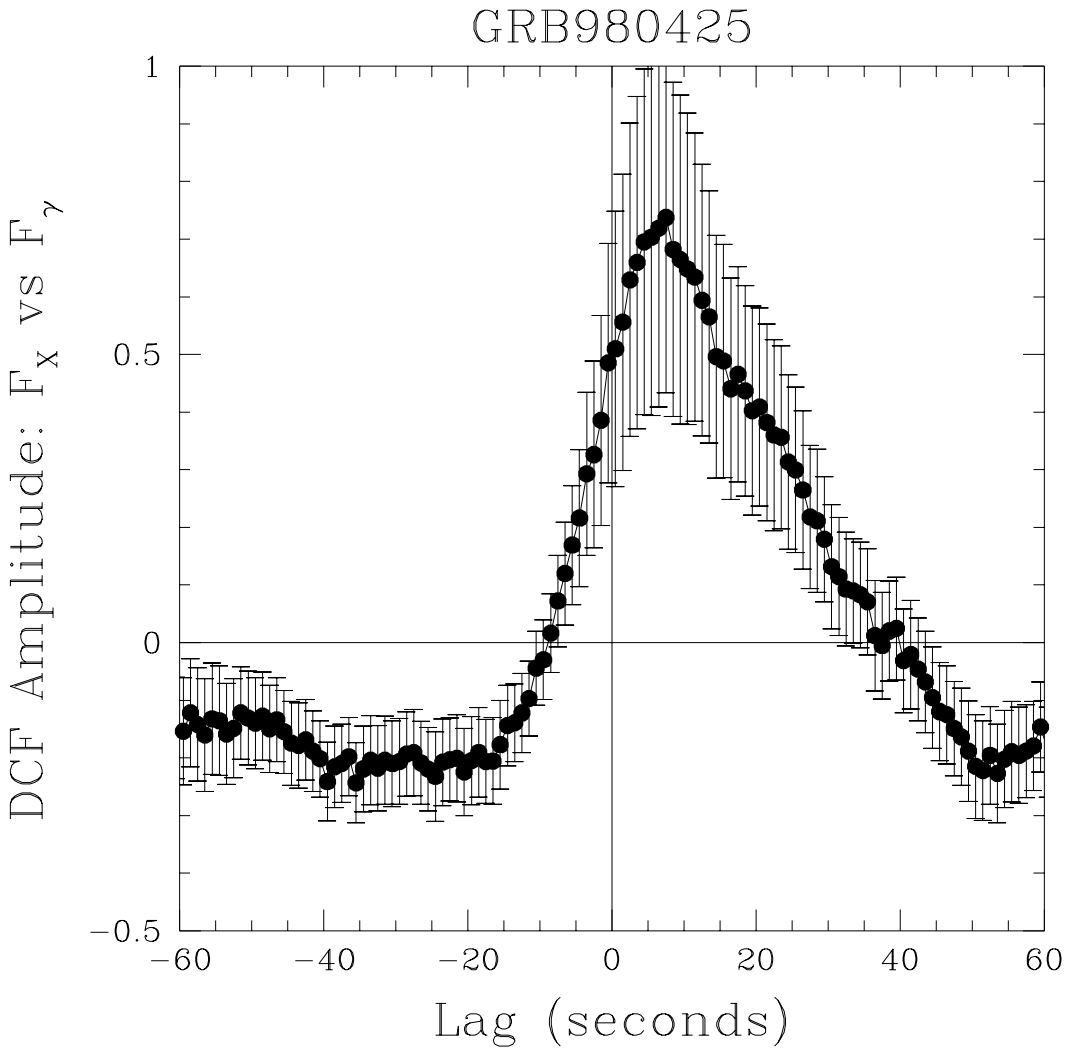

Fig. 2 – Discrete Correlation Function between WFC and GRBM light curves. The maximum at ∼5 seconds indicates positive correlation between the two curves with the WFC light curve lagging the GRBM one by that temporal lag.

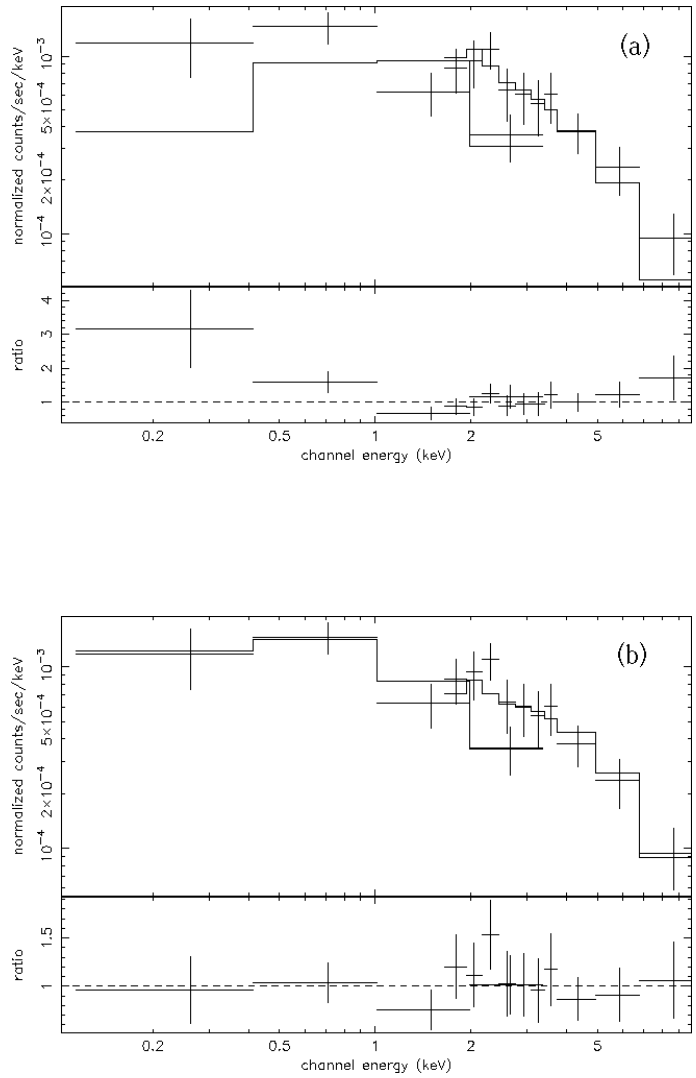

Fig. 4 – BeppoSAX LECS and MECS spectra of S1 fitted with (a) a single power-law and (b) a power-law plus black body. The lower panels show the ratios between the data and the model. See Table 2 for the fit parameters.

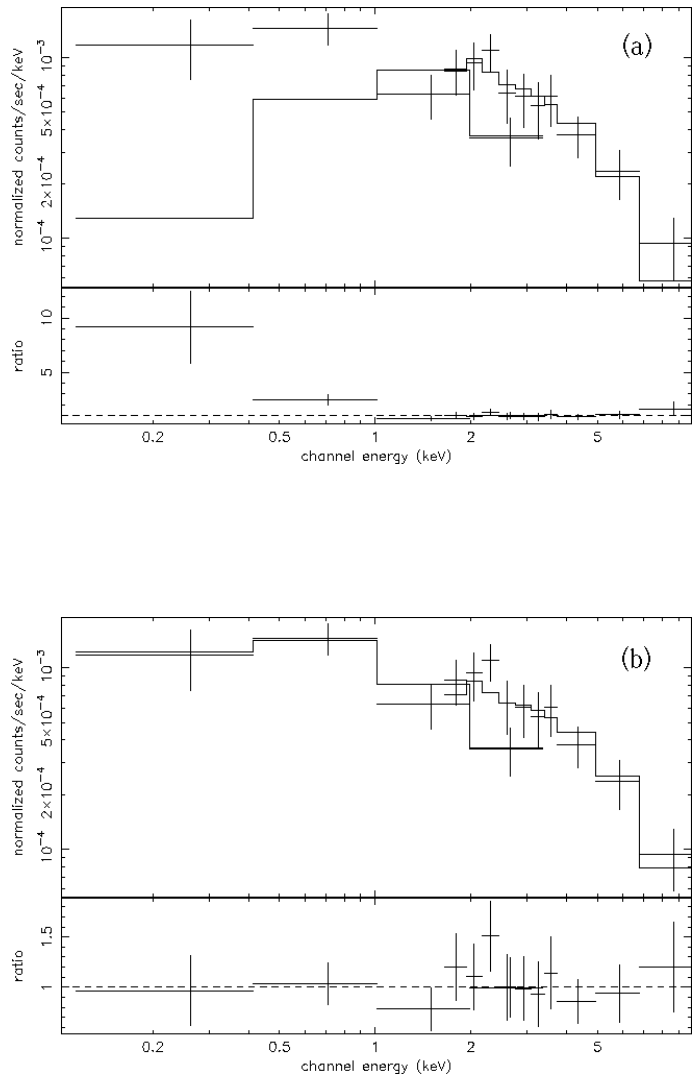

Fig. 5 – BeppoSAX LECS and MECS spectra of S1 fitted with (a) a thermal bremsstrahlung and (b) a thermal bremsstrahlung plus black body. The lower panels show the ratios between the data and the model. See Table 2 for the fit parameters.

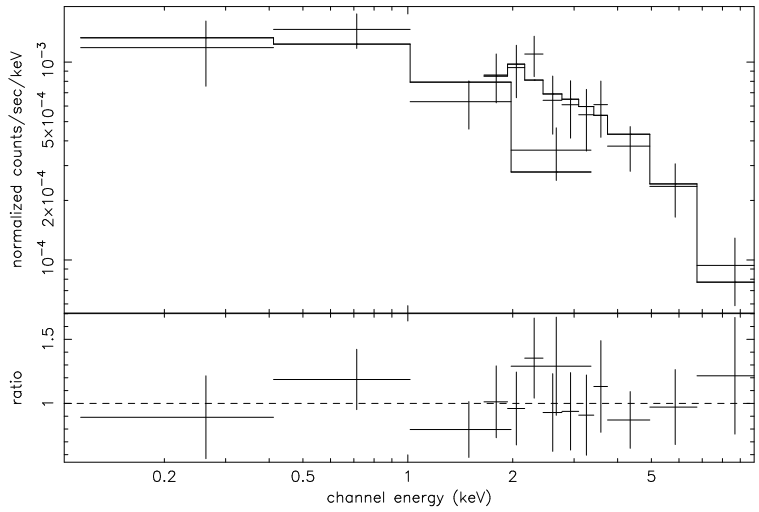

Fig. 6 – BeppoSAX LECS and MECS spectra of S1 fitted with a broken power-law. The lower panel shows the ratios between the data and the model. See Table 2 for the fit parameters.

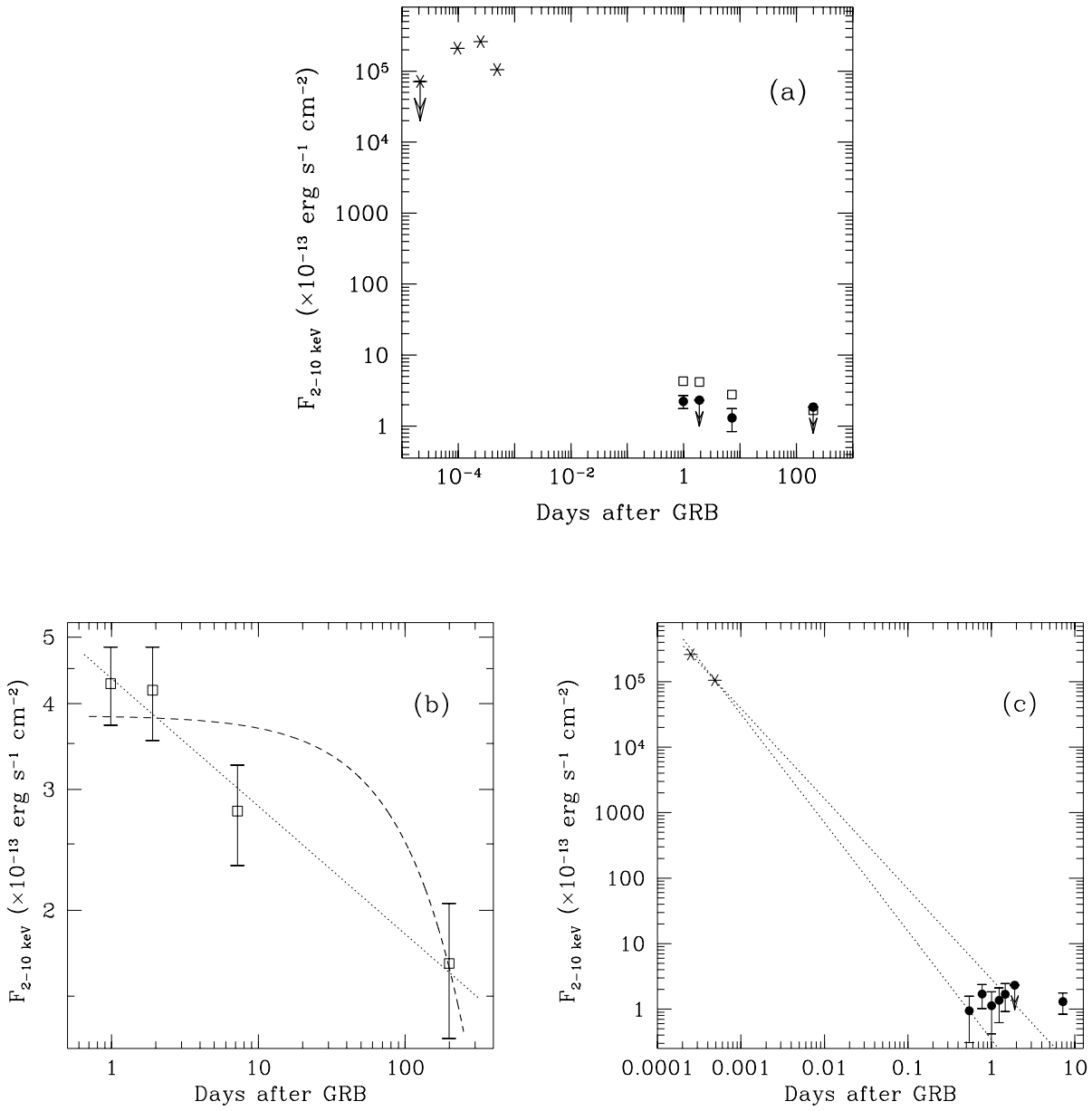

Fig. 7 – BeppoSAX MECS light curves in the 2-10 keV band of the X-ray sources S1 (open squares) and S2 (filled circles) detected in the GRB980425 field. The WFC early measurements in the same band are also shown (stars). Uncertainties for the NFI measurements are 1-σ. The 1-σ error bars for the WFC points are smaller than the symbol size and have not been reported. (b) Same as (a) for source S1 only. The fits to the temporal decay with a power-law of index ~ 0.2 and with an exponential law of e-folding time ~ 500 days are shown as dotted and dashed curves, respectively. (c) Same as (a) for source S2 only. The first NFI measurement of S2 in (a) is replaced here by 5 points obtained by integrating and averaging the flux in shorter time intervals. The dotted lines represent the power-laws of indices $p \simeq 1.6$ and $p \simeq 1.4$ connecting the last WFC measurement and the first and last of the 5 NFI points of the April 26-27 light curve, respectively. The extrapolations of the power-laws to the time of the third NFI observation (May 1998) fall below the lower bound of the data point, although they are compatible with it at the $\gtrsim 2.5\sigma$ level.

This figure "pian_980425_f3a.gif" is available in "gif" format from:

http://arXiv.org/ps/astro-ph/9910235v1


This figure "pian_980425_f3b.gif" is available in "gif" format from:
http://arXiv.org/ps/astro-ph/9910235v1


This figure "pian_980425_f3c.gif" is available in "gif" format from:
http://arXiv.org/ps/astro-ph/9910235v1

This figure "pian_980425_f3d.gif" is available in "gif" format from:

http://arXiv.org/ps/astro-ph/9910235v1